Article

Surface-Modified Garnet Particles for Reinforcing Epoxy Composites

Yiming Jiang [1,2], Fengping Xu [1,3], Kun Liu [1,2,*] and Qiming Feng [1]

[1] School of Minerals Processing and Bioengineering, Central South University, Changsha 410083, China; ymjiang@csu.edu.cn (Y.J.); xufengping@minmetals.com (F.X.); qmfeng@csu.edu.cn (Q.F.)

[2] Hunan Key Lab of Mineral Materials and Application, Central South University, Changsha 410083, China

[3] Hunan Nonferrous Xintianling Tungsten Industry Co. Ltd., Chenzhou 423000, China

* Correspondence: kliu@csu.edu.cn; Tel.: +86-731-8887-7204

check for updates

Abstract: The present study investigated the tribological performance of epoxy (EP) matrix composites enhanced with natural garnet. The garnet was surface-modified with sodium stearate for optimal performance. Composites comprising different contents and particle sizes of modified garnet (MG) were prepared with a mixture of EP and MG. The sodium stearate-bonded garnet and EP formed a stable structure. Tribological performance was measured by a ball-on-plate apparatus under permanent dry sliding conditions and a wear track was obtained by an optical profilometer. The wear mechanism was explored by scanning electron microscopy (SEM) and energy dispersive spectroscopy (EDS) images. Wear test results showed that the coefficient of friction for all EP/MG composites decreased compared with that for neat epoxy. The results also indicated that the addition of MG can evidently improve the tribological properties of EP matrix composites.

1. Introduction

Polymeric materials, such as epoxy (EP), feature a wide range of applications in various industries as substitutes for metals due to their unique mechanical and tribological properties (friction and wear resistance) [1]. Polymeric materials require more in-depth research to ensure their safety and economic and environmental efficiency. Furthermore, defects in cured EP resin have received widespread consideration regarding reinforcement of EP in various conditions, such as coating and wear [2]. EP can be reinforced with rubber, glass fiber, thermoplastic resin, or inorganic particulates [3,4]. Specifically, during the past decades, studies of inorganic particulate-filled EP composites have been carried out to examine their tribological properties [5–7]. Inorganic nanoparticles, as fillers of EP composites, have caught the attention of researchers and engineers [2,8–10]. However, natural inorganic mineral particles used in EP composites remain unappealing, thus limiting their study in this field. Natural particles can potentially have extensive application with their distinctive properties and economic benefits. Therefore, studies should consider the application of natural mineral particles in EP composites.

Substituting other materials, the natural mineral garnet can be used as a reinforcement of EP composite given its excellent physicochemical properties, thermal stability, abundant availability, and desirable ecological alternative [11]. Garnets are nesosilicate minerals with a Moh's hardness of 6.5 to 7.5 [12], which are slightly lower than silicon nitride. Garnet is mainly composed of grossular and exhibits strong chemical stability at high temperatures and its melting point, which can reach 1443–1553 K [12]. Garnet offers good application prospects in the friction field with these excellent properties. Previous research on the application of garnet mainly focused on metal matrix composites [12,13]. These studies showed that the addition of satisfactory particle sizes and amounts of

garnet in Al garnet composite can reinforce its microstructure and microhardness, resulting in drastic improvement of tribological properties. Nevertheless, a wide variety of restrictions and defects led to a narrow range of potential applications. In the field of polymer composites [14,15], as a filler, garnet can significantly promote the tribological properties of EP composite materials to offer significant prospects for their application. Only a few reports considered the natural inorganic mineral as a filler in epoxy composites, thus, it is necessary to understand the tribological properties of garnet composites in some conditions.

In our previous work, we observed that unmodified garnet (unMG) will settle and agglomerate in the matrix, resulting in decreased dispersibility in EP matrix. Therefore, garnet must be surface-modified to improve the dispersion in EP resin. In the present work, we focused on surface modification of natural mineral garnet and understanding the tribological properties of EP composite reinforced with modified garnet (MG) as a low-cost filler material. We considered the effects of particle content and size of garnet in composites on the coefficient of friction and specific wear rate (volume loss at unit load and stroke through continuous rubbing). Four distinct sizes acquired by ultrafine grinding of garnet particles were used to fill the EP matrix with three kinds of gradient contents. Dry sliding wear tests of composite specimens were performed with a ball-on-plate apparatus [9]. Wear tests were carried out at constant parameters and optical profiles of the wear tracks were analyzed with a 3D surface profilometer.

2. Materials and Methods

2.1. Materials

Natural garnet is garnet concentrate with a grade of more than 90%, which was separated and purified from the skarn ore type scheelite by Hunan Nonferrous Xintianling Tungsten Industry Co., Ltd., Chenzhou, China.

The structure of garnet was analyzed with X-ray diffraction (XRD, DX-2700 diffractometer, Haoyuan, Dandong, China). As shown in the XRD pattern of garnet (Figure 1), the main crystalline phase of the specimen is andradite and impurity peaks of the quartz phase are observed [16]. The XRF (Axios mAX, Panalytical, Almelo, The Netherlands) result shows that the garnet specimen is mainly composed of 36.52% of SiO_2, 28.02% of CaO, 11.71% of Fe_2O_3, 8.70% of Al_2O_3, and 1.12% of MgO, which originated from the garnet, and some impurities, such as fluorite, magnetite, quartz, etc. These results indicate the composition of garnet is an andradite-grossular solid solution. Furthermore, the unit cell parameter of the garnet is obtained by structural refinement of XRD data. The unit cell parameter of the andradite-grossular solid solution is determined as a = 11.9601 Å, which is refined by cell refinement of Jade software (MDI, Livermore, CA, USA). According to the variation of unit-cell edges with chemical composition in the garnet group of andradite-grossular (as shown in the Figure 241(g) of [17]), the composition of garnet is an andradite-grossular solid solution of $An_{56}Gr_{44}$. This result was very close to the result from chemical analysis. The chemical formula of the garnet is determined as $Ca_3(Fe_{0.56},Al_{0.44})_2(SiO_4)_3$, which is calculated from the composition of $An_{56}Gr_{44}$ [18]. This finding also shows a difference between the natural garnet used in our investigation and the andradite–grossular garnet and the grossular garnet from other research [19–21].

Commercially available EP resin (E51), accelerator (2,4,6-*tris* (dimethylaminomethyl) phenol), and curing agent (methyl tetrahydrophthalic anhydride) were purchased from Yueyang Dewei Material Co., Ltd., Yueyang, China. Garnet particles as filler with different sizes were surface-modified before mixing with EP resin. Sodium stearate was supplied by Tianjin Kemiou Chemical Co., Ltd., Tianjin, China.
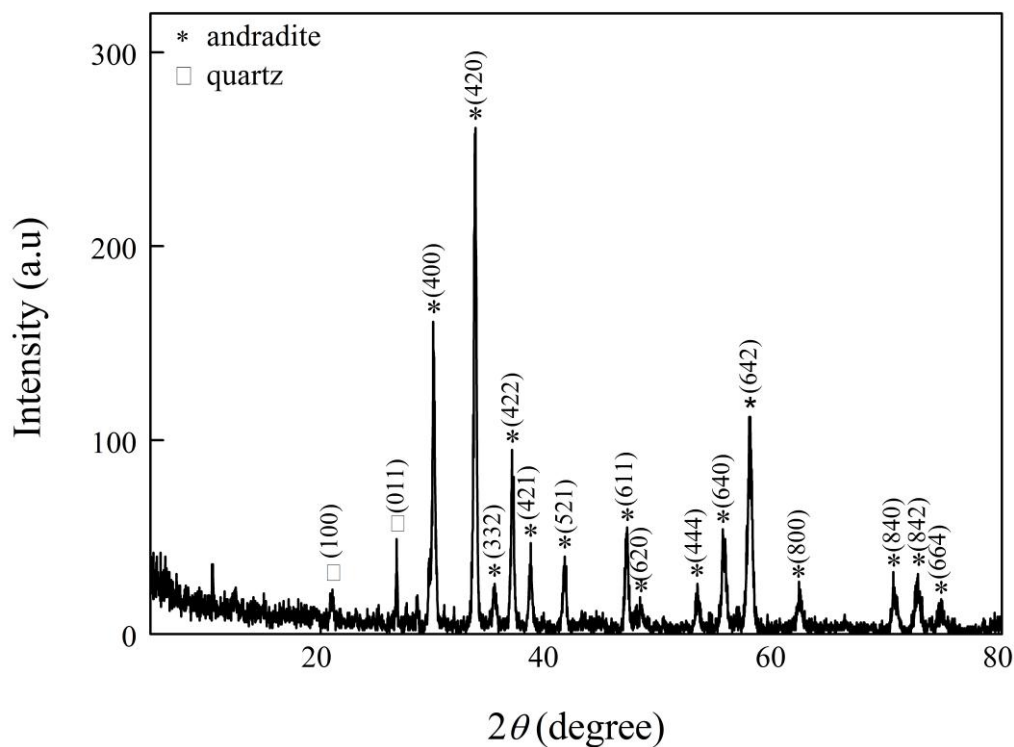
Figure 1. X-ray diffraction pattern of the garnet specimen.

2.2. Ultrafine Grinding and Surface Modification of Garnet

As micron-sized materials have a suitable particle size, the natural garnet was ground to reduce the particle size in advance. Garnet was dispersed in water for grinding by a superfine stirring mill. The suitable parameters were as follows: liquid-to-solid ratio of 2:1, rotational speed of 400 rpm, and duration of 0–300 min. This process produced garnet particle sizes of 4.960–51.884 μm. After ultrafine grinding, garnets with different particle sizes were dispersed in sodium stearate solution and constantly stirred at 400 rpm to achieve surface modification. The reaction temperatures were 50 °C, the content of sodium stearate varied from 0 wt % to 10 wt %, and the liquid-to-solid ratio was 4:1. Four distinct sizes (d_{90}) of MG particles (21.125, 11.300, 8.697, and 4.960 μm) were selected for preparation of EP composites. All MG specimens were stored in desiccators before the preparation of composites.

2.3. Preparation of EP/MG Composites

The EP/MG composites were prepared by directly and thoroughly mixing MG particles and EP with continuous stirring for 30 min. Then, the curing agent and accelerator were injected into the EP mixture for mechanical stirring for 10 min. To prevent the introduction of air and reduce the viscosity of the EP resin, the mixing process was carried out in a vacuum chamber at 75 °C. After mixing, the mixture was poured into a steel mold for curing at 130 °C for 3 h. Following this step, composites were extracted and then cooled down to ambient temperature. Neat epoxy and composites with mass fractions of 10, 20, and 30 wt % of MG were prepared.

2.4. Physicochemical Properties

The properties of garnet changed significantly after surface modification by sodium stearate. In the present research, the water contact angle, infrared spectrum, and surface properties were measured to analyze the effects of modification.

The MG surface is nonpolar. This property induces MG to an activated state. Thus, MG can float on water. Settling experiments showed that up to 96.7% of garnets can suspend stably on the surface of water. This result shows that stearate was successfully grafted to garnet.

The contact angle was investigated using a contact angle measuring instrument (Attension, Biolin, Espoo, Finland). Static contact angles were measured in ambient conditions with a camera by applying the Young-Laplace equation. A drop of deionized solvent (4 µL) from an injector was dripped on the surface of the specimens. Two kinds of solvent, ultrapure water and benzene containing 2 wt % epoxy, were used for this test. Five measurements were performed to acquire the average value of the contact angle.

Structural analyses of MG, unMG, and sodium stearate were conducted with a Nexus (Nicolet, Waltham, MA, USA) Fourier transform infrared spectrometer (FTIR). The results were used to identify the peaks for each functional group of specimens. Structural change in MG can be characterized by change in functional groups. Surface properties of the surface area and pore properties were determined with an Autosorb-1 automatic apparatus (Quantachrome, Boynton Beach, FL, USA) from N_2 adsorption isotherms.

The dispersion of unMG and MG particles in epoxy was investigated with an Axiovert 200 MAT (Zeiss, Oberkochen, Germany) optical microscopy. The composites containing the same content of unMG and MG were prepared for the test, respectively. All the specimens were polished before testing.

2.5. Wear Test and Tribological Characterization

A UMT-3H (Cetr, Campbell, CA, USA) ball-on-plate test system was used to investigate the friction and wear behavior (wear resistance and mechanism) of neat EP and EP/MG composite by sliding against a ball of silicon nitride (Si_3N_4) with a linear motion, as shown in Figure 2. The silicon nitride ball (9 mm) was continuously and reciprocally slid against the stationary specimen in ambient conditions under the same parameters of constant velocity of 1.2 cm/s and applied normal load of 150 N for 1 h. Before the test all specimens were polished against SiC sandpaper to ensure proper contact of the counterface (contact surface of composite and Si_3N_4). The surfaces of both the specimen and the ball were cleaned with ethanol and thoroughly dried before the tests. The size of the specimen was 20 mm × 20 mm × 5 mm. The wear scar width and depth of the EP and EP/MG composite were determined by an NPFLEX 3D (Bruker, Billerica, MA, USA) surface profilometer.
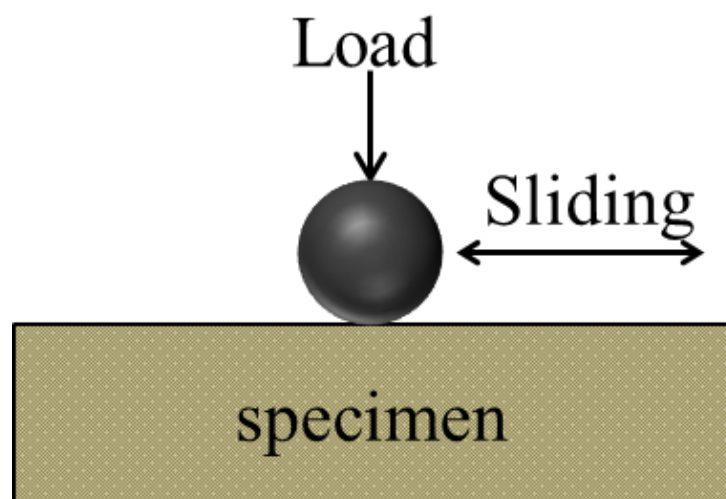

Figure 2. Schematic diagram of the wear test.

Scanning electron microscopy (SEM, NanoSEM, FEI, Hillsboro, OR, USA) was used to observe the original surface and worn tracks. Surfaces of specimens were sprayed with a thin gold coating for observation of the wear mechanism.

The specific wear rate W_r of the specimen was calculated by the Equation (1) [22,23]:

$$W_r = \frac{V}{D \times L} \text{ mm}^3/\text{Nm } (V = S \times d) \tag{1}$$

where V, D, L, S, and d correspond to the wear volume, applied normal load, total sliding distance, cross sectional area, and sliding stroke, respectively.

3. Results and Discussion

3.1. Physicochemical Properties of MG

Garnet showed a strong hydrophilic surface that led to poor compatibility between itself and the matrix. Therefore, the hydrophilic surface of garnet powder must be modified to become oleophilic before preparation of composite materials. MG surface became nonpolar, which contributed to extreme hydrophobicity and lipophilicity. As a consequence, the contact angle (Figure 3) exhibited remarkable variations due to surface modification with sodium stearate.
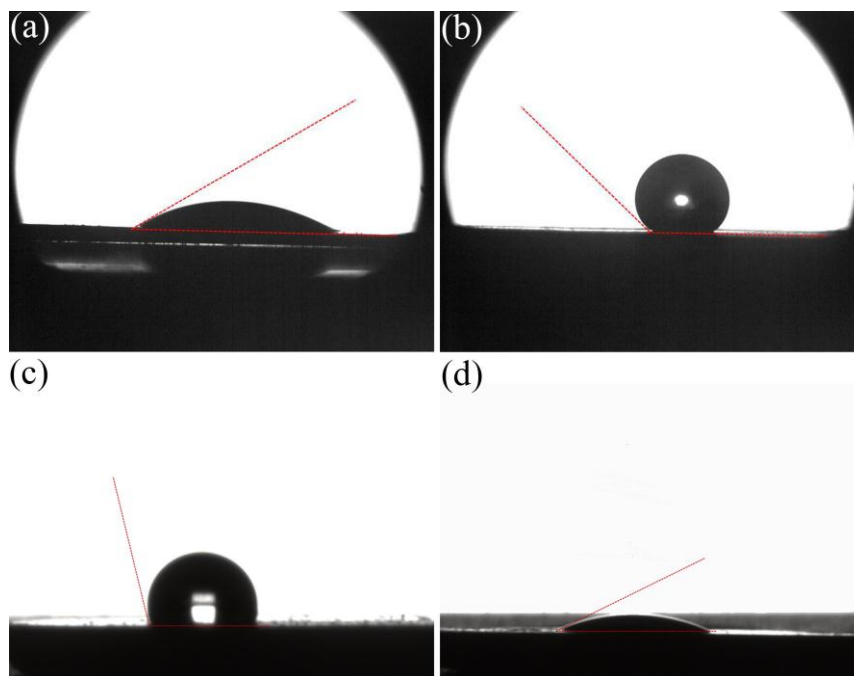

Figure 3. Contact angle of: (**a**) unMG in water; (**b**) MG in water; (**c**) unMG in benzene containing 2 wt % epoxy; and (**d**) MG in benzene containing 2 wt % epoxy.

As shown in Figure 3, contact angles of unMG and MG in water were approximately 20° and 135°, respectively. At the same time, contact angles of unMG and MG in benzene containing 2 wt % epoxy were 104° and 23°, respectively. This result indicates that unMG exhibited strong hydrophilicity and oleophobicity, whereas MG was extremely hydrophobic and lipophilic. The water contact angle of MG is larger than the 82.03° angle of EP [23]. The significant transformation of the contact angle confirms the successful grafting of sodium stearate on the surface of the garnet. Sodium stearate, with its excellent surface activation effect, remarkably enhances the hydrophobic properties of garnet. Compared with modification of nanoparticles [24,25], MG microparticles had a higher water contact angle.

Figure 4 shows the FTIR spectra of unMG and MG. The garnets before and after modification exhibited the same stretching vibration bands at 1463.3, 913.5, 849.0, 690.3, 526.8, and 461.1 cm^{-1} [26–29]. These two specimens also showed the –OH band at 3370 cm^{-1}. MG bands at 2918 cm^{-1} and 2849 cm^{-1}

resulted from, respectively, asymmetric and symmetric stretching vibration of methylene [24,30], indicating successful loading of sodium stearate ions into the garnet. The bands at 1434, 1464, and 1558 cm^{-1} of sodium stearate were attributed to vibration absorption of methyl and methylene, and asymmetric stretching vibration of the carboxylate group, respectively [30–32]. When sodium stearate was grafted onto the garnet, those bands interacted with the band at 1445 cm^{-1}, leading to a band shift, demonstrating chemical adsorption of sodium stearate in garnet. Stearate radicals reacted with Ca^{2+} and Fe^{3+} of garnet and formed a hydrophobic structure on the garnet surface.
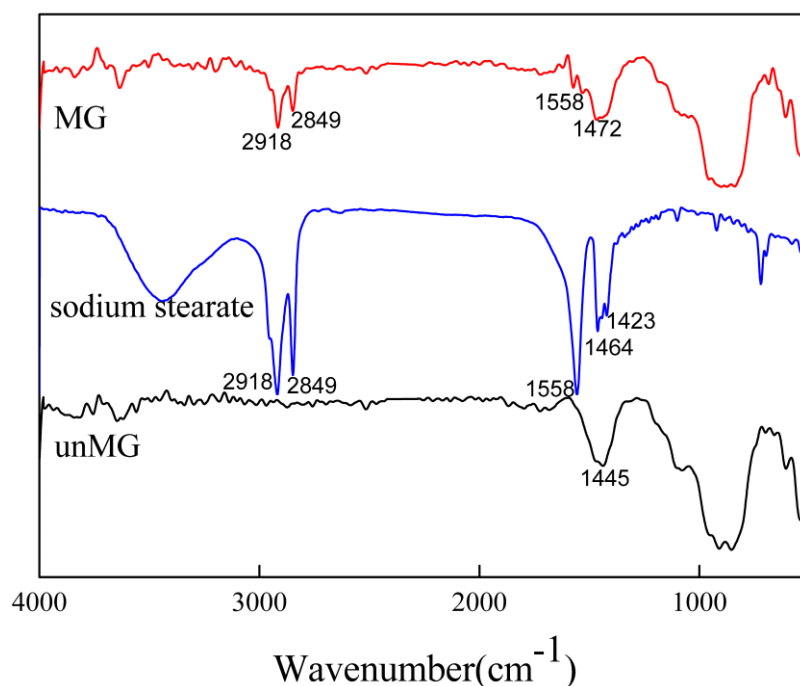
Figure 4. The FTIR spectra of the garnet before and after modification.

Figure 5 displays nitrogen adsorption-desorption isotherms of unMG and MG. The rectangle inset in Figure 5 shows the corresponding pore size distributions, which were calculated by the desorption branch with the Barrett-Joyner-Halenda method. Nitrogen adsorption isotherms of unMG and MG showed a typical type II adsorption isotherm with a type H3 hysteretic loop [33,34]. Adsorption capacity still rapidly increased at high relative partial pressure (P/P$_0$) of more than 0.9, and limiting adsorption was not observed, indicating that it is a typical hysteretic loop of type H3. The hysteretic loop of type H3 manifested aggregates of plate-like particles, leading to slit-shaped pores. As shown in the inset, a relatively narrow and bimodal porous structure appeared in unMG and MG specimens. Pore size distribution of MG was much wider. The unMG featured two narrow peaks, ranging from 14 to 33 nm and 33 to 47 nm. This result indicates uniform pore size distribution of unMG. A stronger broad peak of MG appeared at 16–37 nm. This finding suggests that unMG mainly contained mesopores, and such a pore structure was not changed with modification. The MG exhibited broad peaks, ranging from 37 to 91 nm. A drastic decrease in pore volume occurred at 33–37 nm. This result indicates that stearic acid ions dispersed in, and occupied, the mesopores and macropores of garnet. The formation of macropores is probably attributed to extraction of physically absorbed stearic acid ions [35].
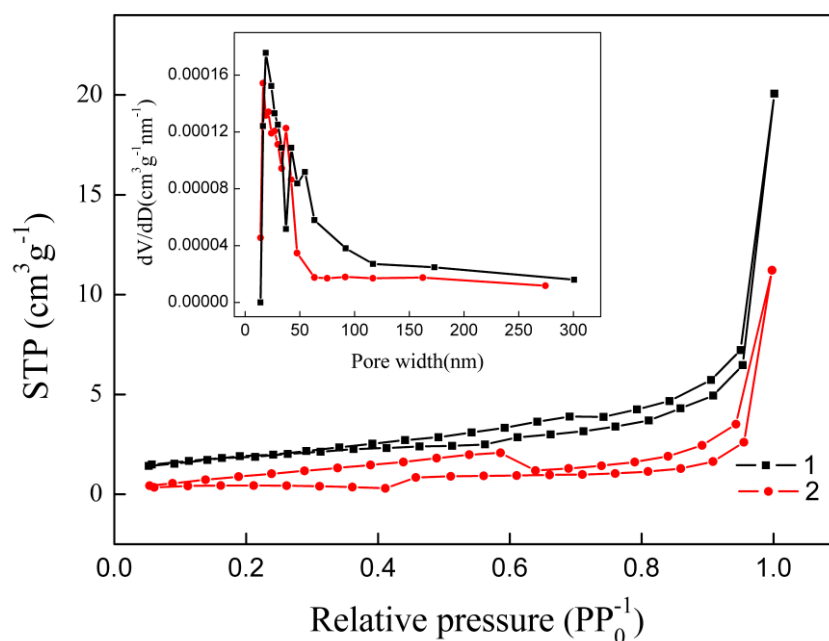
Figure 5. The nitrogen adsorption-desorption isotherms of the MG (1) and unMG (2). The rectangle inset shows corresponding pore size distributions.

Brunauer-Emmett-Teller surface area of garnets before and after modification reached 1.444 and 6.228 m^2/g, respectively. The increased surface area of garnet after modification explains the better dispersion of MG microparticles [33]. Surface energy of unMG is relatively high: according to the principle of minimum energy, unMG particles will aggregate to reduce surface energy [36]. Therefore, a serious reunion phenomenon occurred among garnet particles. Large unMG particles are formed due to agglomeration, which reduces the surface area of garnet. On the contrary, MG was coated with a layer of stearic acid radicals, which reduced the surface energy and put the particles in a stable dispersion state [37]. Thus, MG showed better dispersibility and caused an increase in surface area compared with unMG.

The above results indicate that sodium stearate was successfully grafted onto the garnet. Then hydroxyl groups contributed to improve the dispersion of MG in epoxy. We analyzed the dispersion of unMG and MG particles in epoxy by optical microscopy, as shown in Figure 6. Figure 6a shows serious agglomeration of unMG particles. On the contrary, MG in composite (Figure 6b) displays better dispersion, which will help to improve the tribological performance of the EP/MG composite.
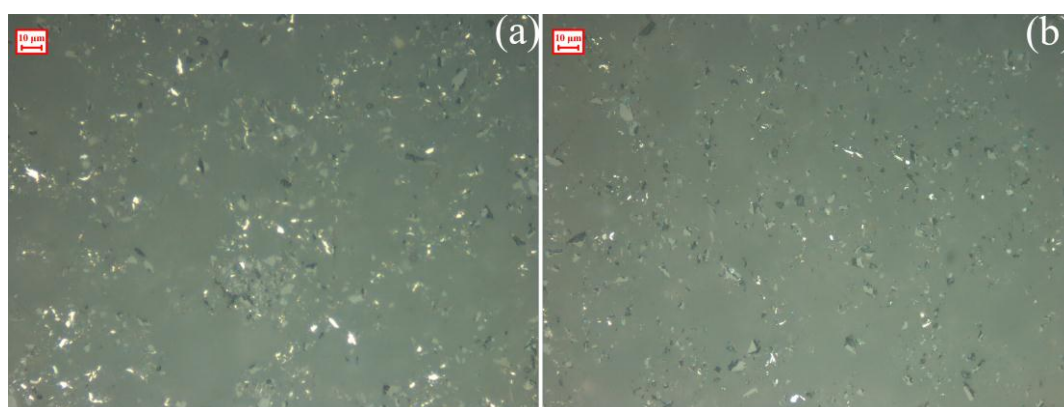
**Figure 6.** Optical microscopy images of particles in composite: (**a**) unMG; and (**b**) MG.

3.2. Tribological Characterization and Wear Mechanisms

In ball-on-plate tests, the reciprocating ball continuously slides against the stationary surface of the specimen. Given that garnet is a promising, naturally wear-resistant material, especially with the remarkable compatibility of MG surface with EP resin, studies should investigate the tribological performance of EP/MG composite. In the present study, experiments were performed to determine the effects of content and size of garnet microparticles on the tribological properties of EP/MG composite.

3.2.1. Effects of Content and Particle Size of MG on Coefficient of Friction

Variations in coefficient of friction of neat EP and EP/MG composite with different particle sizes and contents at constant parameters, including an applied normal load of 150 N and sliding velocity of 1.2 cm/s, are displayed in Supplementary Materials Figure S1(1–13). As shown in these figures, all specimens underwent two stages: a running-in period and a stable state, as studied in references [10,38]. In the running-in period, the coefficient of friction of all specimens increased with the increasing time at the initial stage. Different specimens have different rate of increase of coefficient of friction. After the specimens completed the running-in period, a stable period was reached when coefficient of friction remained at a substantially stable level for almost all composites, as exhibited in the supplementary materials. A slight variation in the coefficient of friction of these composite specimens was observed after reaching the stable state. However, a fluctuation was detected in the coefficient of friction of neat EP and composites with 8.697 μm particle size of MG. A significant decrease was observed after the stable stage of EP/MG composite with a particle size of 8.697 μm, and this result can be ascribed to the development of a transfer film [39]. The EP/MG composite presented a better capacity to form a transfer film on the surface of the composite and counterpart of the Si_3N_4 ball in wear test; this condition can avoid plow and reduce the coefficient of friction with lubrication of the transfer film [39,40].

The rate of increase of the coefficient of friction for different specimens is quite different. As shown in Figure S1(2,5–9,11), these composites have a greater increased rate of coefficient of friction in the running-in period, compared with other composites and neat epoxy. This result was understandable at early stages, where the original surfaces of these composite specimens and the Si_3N_4 ball were rougher, resulting in high coefficients of friction, as shown in Figure 7a. The results are in accord with the hypothesis that numerous asperities are present on the surface of composites. Thus, the real contact area between these composites and Si_3N_4 ball is small, leading to strong interlocking [1,38]. Interlocking resulted in large contact pressure, which would cause a rapid increase in the coefficient of friction of these specimens. As shown in Figure 7b, the original surface of EP was smoother, resulting in a lower coefficient of friction in the initial stage.
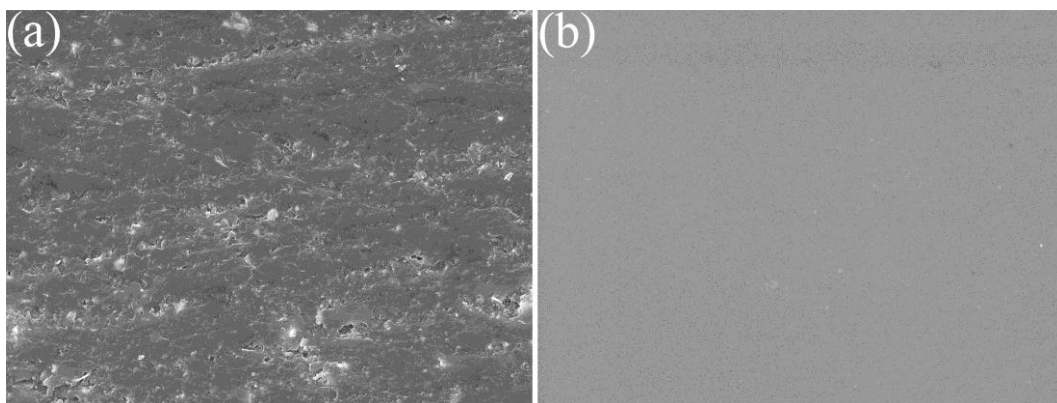
Figure 7. SEM images of the original surface of specimens: (**a**) EP/MG composite containing 10 wt % MG with particle size 8.697 μm; and (**b**) neat EP.

For in-depth investigation, the effects of the content and particle size of MG in the composite on the coefficient of friction were investigated, and the results are displayed in Figure 8. Each value of the coefficient of friction is the average value of the stable state and is based on low standard deviation. As presented in Figure 8, the coefficient of friction of all EP/MG composites was decreased compared with that of neat EP. However, the magnitude of reduction differed. This result indicates that the addition of MG filler contributed to the decrease in coefficient of friction [3]. This can be attributed to the MG can improve the hardness and resistance of decomposition of composite, compared with neat EP [23]. Contact temperature is another significant factor that impacts the coefficient of friction [41]. Incorporating MG reduces the contact temperature. High contact temperature of neat EP led to severe softening of the resin matrix during friction, which increased the coefficient of friction. The coefficient of friction of composites containing 10 wt % MG experienced the lowest coefficient of friction. A trend toward an increased coefficient of friction was observed when the content of MG totaled 20 and 30 wt %. This result shows that composites containing 10 wt % of MG provided a better effect on decreasing the coefficient of friction. In this condition, less MG content in the composite resulted in better dispersion and bonding in the resin matrix than high MG content. This situation can promote the development of thin and uniform adhering transfer films on the counterpart surface [39,42].
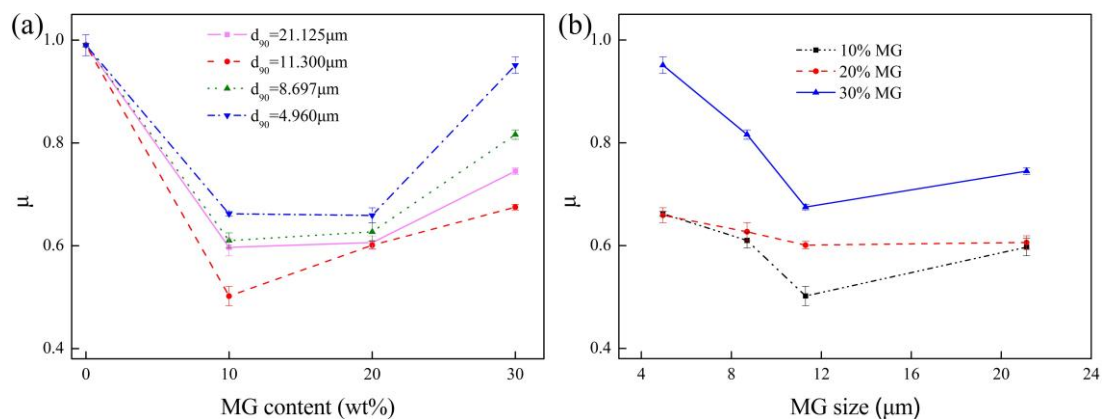
Figure 8. Effect of content (**a**) and particle size (**b**) for MG in composites on the coefficient of friction.

As shown in Figure 8b, the coefficient of friction of the EP/MG composite assumes an obvious decrease with increasing particle size from 4.960 μm to 11.300 μm. With a further increase in particle size up to 21.125 μm, the coefficient of friction increases for all the composites. The smallest coefficient of friction was observed for EP/MG composite at a particle size of 11.300 μm. The composite containing 4.960 μm MG obtained the poorest efficiency in decreasing the coefficient of friction. This result can be explained by the severe agglomeration of microparticles measuring 4.960 μm; there was high surface roughness at the contact surface, which led to an increase in the coefficient of friction [43].

Figure 9 illustrates the synergistic effect of content and particle size of MG in composite on the coefficient of friction. The composite containing 10 wt % MG with a particle size of 11.300 μm demonstrated the highest decrease in the coefficient of friction. Uniform dispersion of MG particles and strong matrix bonding are considered to promote tribological properties [1]. However, when the content and particle size of microparticles were beyond the suitable range, agglomeration of microparticles gave rise to an increase in particle size and the number of regions (without MG) with low hardness. The optimal content and size of MG particles provides the best support for the sliding load and are similar to those of ZrB_2 microparticles [44].
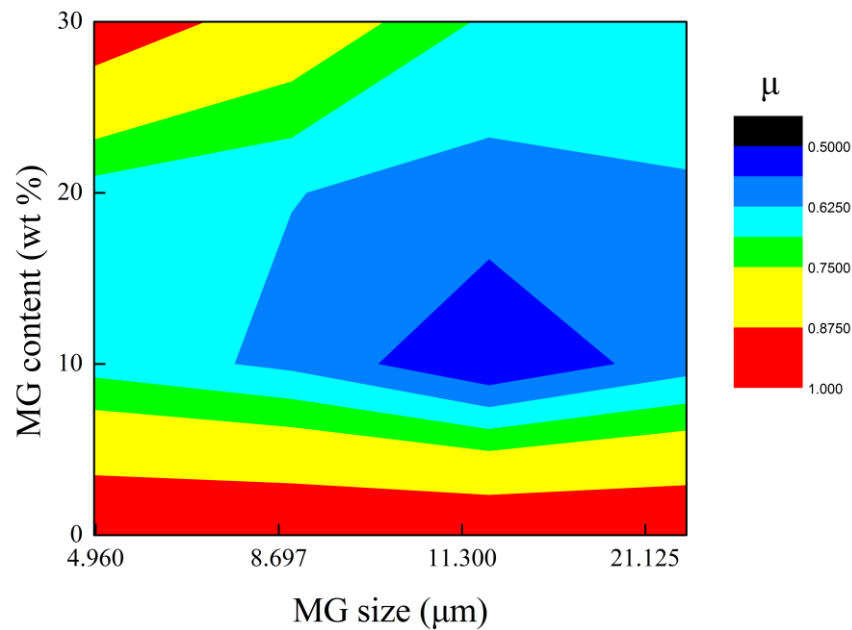
Figure 9. Contour graph of effect of MG content and particle size on the coefficient of friction for composites.

3.2.2. Effects of Content and Particle Size of MG on Specific Wear Rate

Supplementary Materials Figure S2(1–13) present the optical profiles of the wear tracks and line scans of the cross-profiles on the neat EP and EP/MG composites with measurements. A remarkable groove on the surface was observed in the 3D optical profiles of all composites and neat EP. The width and depth of the groove significantly differed for various specimens. As shown in Figure S2(1b–13b), the depth of the wear track was larger in the center than on the edge, suggesting that the abrasive wear (epoxy stuck to the surface of the Si_3N_4 ball) in the center was the most severe compared with that on the edge. This result is attributed to the abrasion with reciprocating sliding against the Si_3N_4 ball.

Line scans of the cross-profiles in Figure S2(1c–13c) display a variation in wear depth as a function of wear width, which was obtained with the line scan from the cross-section of the wear track, as shown by the dotted line in the planform. The cross-sectional area of the wear track was calculated by integration of the data of the line scan. The cross-sectional area of the composite filled with the most appropriate MG was smaller than that of the neat EP. The cross-sectional area was multiplied by the length of wear track to calculate the wear volume.

Figure 10 shows the effects of content and particle size for MG in composite on specific wear rate. The specific wear rate was computed by Equation (1). As shown in Figure 10a, the specific wear rate of composites was increased with increasing MG (4.960 and 21.125 μm) content from 10 wt % to 20 wt %. Then the specific wear rate of these composites was decreased with the further increase of MG content to 30 wt %. The specific wear rate of composites displayed the opposite variation with the addition of MG of 11.300 μm. There were no regular variations in specific wear rate of composites with the variation of MG (8.697 μm) content. However, only two composites containing 10 wt % MG (8.697 and 11.300 μm) had lower specific wear rates than EP. Compared with neat EP, the specific wear rate of these composites was reduced by 18.2% and 14.3%, respectively. This result demonstrated that only appropriate particle size benefits reduction of specific wear rate. The MG (8.697 and 11.300 μm) exhibited better dispersion and helped to strengthen the interface bonding between the particles and epoxy, contributing to an enhancement of wear resistance. In this condition, transfer film composed of MG and EP matrix forming on the counterface helped to decrease the specific wear rate. As shown in Figure 10b, the specific wear rate of composites containing 10 and 20 wt % MG displayed an obvious V-shaped trend. The specific wear rate of the composite decreased with increasing MG (10 wt %)

particle size from 4.960 μm to 8.697 μm. The specific wear rate of the composite decreased with increasing MG (20 wt %) from 4.960 μm to 11.300 μm. The specific wear rate of these composites both increased with a further increase in particle size. The specific wear rate of composites displayed the opposite variation with the addition of MG (30 wt %). The EP/MG composite (10 wt % MG) with a particle size of 8.697 μm revealed the lowest specific wear rate compared with other specimens, thus providing the best wear resistance. As for other composites, inappropriate particles were agglomerates, which led to high roughness and drastic abrasive wear, according to research on hexagonal boron nitride [5]. Then aggregate abrasive particles were dug out and the matrix was desquamated, which increased the specific wear rate.
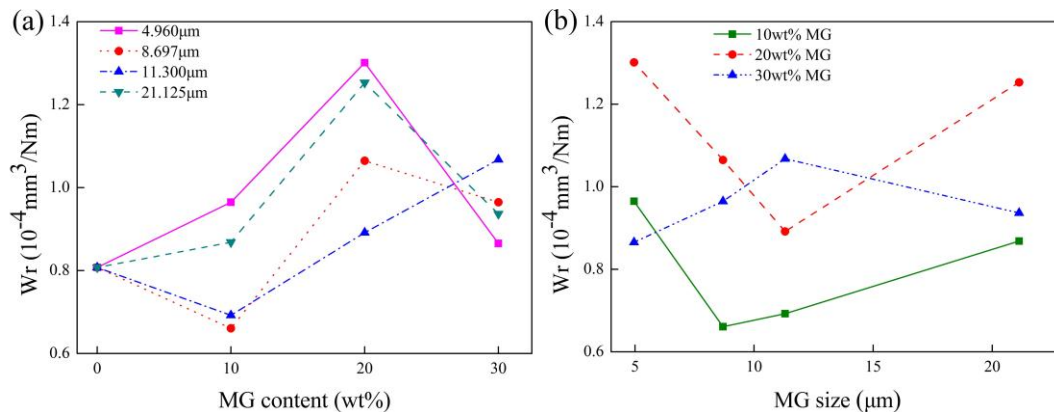

Figure 10. Effect of content (**a**) and particle size (**b**) for MG in composite on the specific wear rate.

3.2.3. Wear Mechanisms

In order to study the wear mechanism of composites, we analyzed the morphology of the worn surface. As represented in Figure 11, various cracks formed on the surfaces of neat epoxy and the EP/MG composite. The cracks were perpendicular to the sliding direction, resulting from the brittle character of EP under loading. The varying degrees of surface fluctuation were attributed to adhesion of epoxy to the surface of the Si_3N_4 ball, consequent plastic deformation, and separation of epoxy debris by friction. The surface fluctuation of the composite was slighter than EP, as shown in Figure 11a,b. Compared with pure EP, a large number of wear debris appeared near the crack of the composite surface, which was caused by abscission of garnet (Figure 11b). This result was due to the weak wear resistance of the resin and decreased bonding of particles to the matrix [39]. Numerous microcracks were present in the composite surface, as shown in Figure 11d. Microcracks can be conducive to reducing the specific wear rate, because they can absorb impact energy when separating the epoxy. Additionally, MG could resist the spread of the crack, as shown in the rectangle in Figure 11d, because the cracks were deflected and dissipated when they encountered MG particles. Figure 12 shows visible cracks of composites, which were mainly caused by digging out of agglomeration of MG particles. This result indicated that the agglomeration of particles would cause a severe destruction of EP [45].

SEM-EDS images of the wear debris on the worn surface are shown in Figure 13. There were C, O, Si, and Ca elements in the wear debris, indicating that the wear debris was the composite that broke off from the surface. Therefore, it was speculated that MG particles were wrapped in resin and were dug out from the surface during friction, which indicates the strong bonding between particles and epoxy.
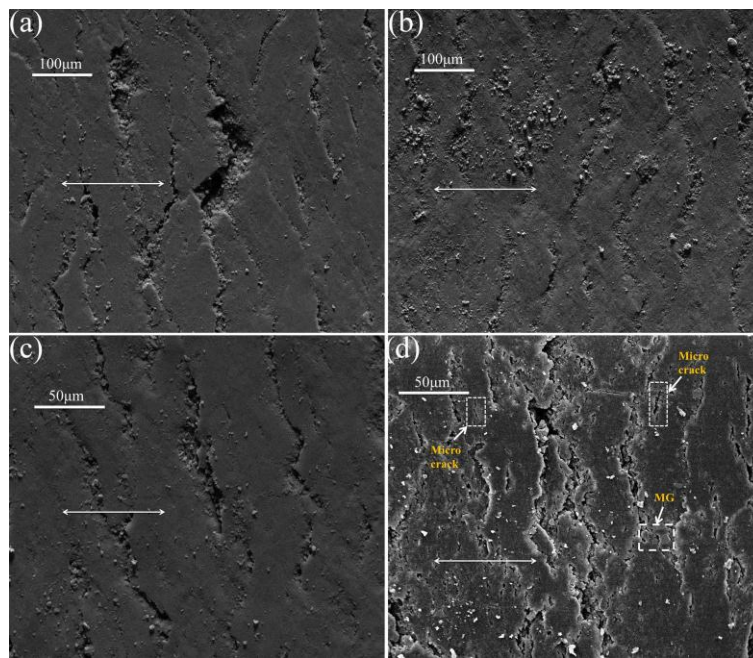
Figure 11. SEM micrographs of the worn surfaces of specimens: (**a**,**c**): neat epoxy; and (**b**,**d**): EP/MG composite. The arrows indicate the sliding direction.
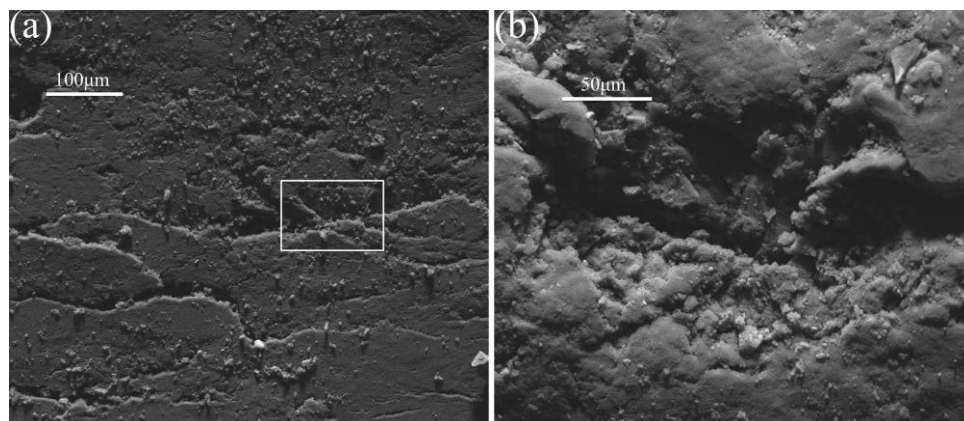
Figure 12. SEM micrograph (**a**) and magnified micrograph (**b**) of the wear crack of the EP/MG composite.
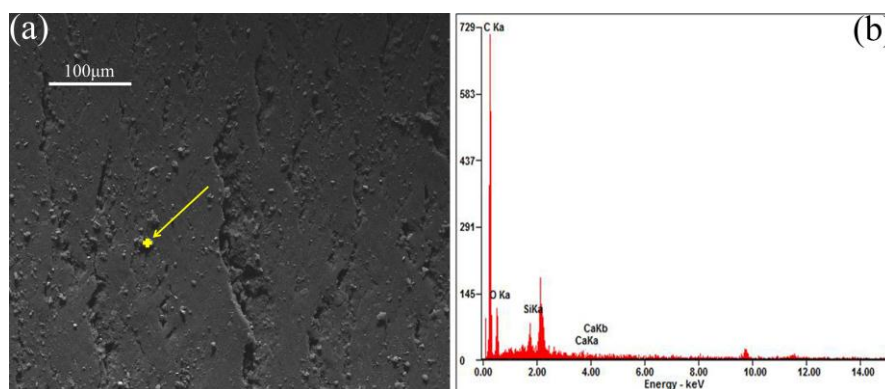
Figure 13. SEM micrograph (**a**) and EDS analysis (**b**) of wear debris of the EP/MG composite.

4. Conclusions

In the present paper, the preparation and tribological properties of EP composite filled with MG particles with different contents and particle sizes were systematically researched at constant parameters. The contact angle in water and benzene were significantly improved with surface modification by sodium stearate, reaching 135° and 37°, respectively. The surface area of garnet also increased, from 1.444 to 6.228 m^2/g, through surface modification. The results prove that the hydrophilic surface properties of garnet became extremely hydrophobic. Surface modification greatly improves the dispersion of garnet in epoxy. According to the results of the wear test, the addition of MG to EP can effectively promote tribological properties. This condition indicates that surface modification contributes to strengthening interfacial interactions between microparticles and matrix resin. The EP/MG composite containing 10 wt % MG with a particle size of 11.300 μm exhibited the best tribological properties compared with neat EP and other composites. This composite presented the lowest coefficient of friction and specific wear rate. Both particle size and content of MG affect the tribological properties of EP/MG composite. EP/MG composites with different MG contents can decrease the coefficient of friction. However, only systems with appropriate content (10 wt %) and particle size (8.697 and 11.300 μm) exhibit an improvement of wear resistance.

Supplementary Materials: The following are available online at http://www.mdpi.com/2075-163X/8/5/217/s1: Figure S1. Variations of the coefficient of friction with sliding time for epoxy (EP)/modified garnet (MG) composites and neat epoxy; Figure S2. Optical profiles of wear tracks on EP/MG composites and neat epoxy resin: (a) 3D profile; (b) planform; and (c) line scan of the cross-profile.

Author Contributions: Kun Liu and Qiming Feng conceived and designed the experiments; Yiming Jiang and Fengping Xu performed the experiments and analyzed the data; and all the authors wrote the manuscript.

Conflicts of Interest: The authors declare no conflict of interest.

References

1. Chauhan, S.R.; Thakur, S. Effects of particle size, particle loading and sliding distance on the friction and wear properties of cenosphere particulate filled vinylester composites. *Mater. Des.* **2013**, *51*, 398–408. [CrossRef]
2. Han, W.; Chen, S.; Campbell, J.; Zhang, X.; Tang, Y. Fracture toughness and wear properties of nanosilica/epoxy composites under marine environment. *Mater. Chem. Phys.* **2016**, *177*, 147–155. [CrossRef]
3. Chang, L.; Zhang, Z. Tribological properties of epoxy nanocompositesPart II. A combinative effect of short carbon fibre with nano-TiO_2. *Wear* **2006**, *260*, 869–878. [CrossRef]
4. Zhang, Z.; Breidt, C.; Chang, L.; Haupert, F.; Friedrich, K. Enhancement of the wear resistance of epoxy: Short carbon fibre, graphite, PTFE and nano-TiO_2. *Compos. Part A Appl. Sci. Manuf.* **2004**, *35*, 1385–1392. [CrossRef]
5. Kadiyala, A.K.; Bijwe, J. Surface lubrication of graphite fabric reinforced epoxy composites with nano- and micro-sized hexagonal boron nitride. *Wear* **2013**, *301*, 802–809. [CrossRef]
6. Rong, M.Z.; Zhang, M.Q.; Shi, G.; Ji, Q.L.; Wetzel, B.; Friedrich, K. Graft polymerization onto inorganic nanoparticles and its effect on tribological performance improvement of polymer composites. *Tribol. Int.* **2003**, *36*, 697–707. [CrossRef]
7. Xing, X.S.; Li, R.K.Y. Wear behavior of epoxy matrix composites filled with uniform sized sub-micron spherical silica particles. *Wear* **2004**, *256*, 21–26. [CrossRef]
8. Aliofkhazraei, M.; Moradi, M.H.; Toorani, M.; Golgoon, A.; Rouhaghdam, A.S. SiAlON-epoxy nanocomposite coatings: Corrosion and wear behavior. *J. Appl. Polym. Sci.* **2016**, *133*, 43855. [CrossRef]
9. Esteves, M.; Ramalho, A.; Ferreira, J.A.M.; Nobre, J.P. Tribological and mechanical behaviour of epoxy/nanoclay composites. *Tribol. Lett.* **2013**, *52*, 1–10. [CrossRef]
10. Neitzel, I.; Mochalin, V.; Bares, J.A.; Carpick, R.W.; Erdemir, A.; Gogotsi, Y. Tribological properties of nanodiamond-epoxy composites. *Tribol. Lett.* **2012**, *47*, 195–202. [CrossRef]

11. Sharma, A.; Arora, R.; Kumar, S.; Singh, G.; Pandey, O.P. Wear performance of garnet aluminium composites at high contact pressure. In Proceedings of the International Conference on Condensed Matter & Applied Physics, Bikaner, India, 30–31 October 2015.

12. Sivakumar, S.; Padmanaban, K.; Uthayakumar, M. Wear behavior of the Al (LM24)-garnet particulate composites under dry sliding conditions. *Proc. Inst. Mech. Eng. Part J J. Eng.* **2014**, *228*, 1410–1420. [CrossRef]

13. Sharma, A.; Kumar, S.; Singh, G.; Pandey, O.P. Effect of particle size on wear behavior of Al–Garnet composites. *Part. Sci. Technol.* **2014**, *33*, 234–239. [CrossRef]

14. Bhimaraj, P.; Burris, D.L.; Action, J.; Sawyer, W.G.; Toney, C.G.; Siegel, R.W.; Schadler, L.S. Effect of matrix morphology on the wear and friction behavior of alumina nanoparticle/poly(ethylene) terephthalate composites. *Wear* **2005**, *258*, 1437–1443. [CrossRef]

15. Jiguet, S.; Judelewicz, M.; Mischler, S.; Hofmann, H.; Bertsch, A.; Renaud, P. SU-8 nanocomposite coatings with improved tribological performance for MEMS. *Surf. Coat. Technol.* **2006**, *201*, 2289–2295. [CrossRef]

16. Antao, S.M. Three cubic phases intergrown in a birefringent andradite-grossular garnet and their implications. *Phys. Chem. Miner.* **2013**, *40*, 705–716. [CrossRef]

17. Deer, W.A.; Howie, R.A.; Zussman, J. *Rock Forming Minerals, Volume 1A: Orthosilicates*; The Geological Society: London, UK, 1982; p. 488.

18. Antao, S.M.; Klincker, A.M. Origin of birefringence in andradite from Arizona, Madagascar, and Iran. *Phys. Chem. Miner.* **2013**, *40*, 575–586. [CrossRef]

19. Antao, S.M.; Klincker, A.M. Crystal structure of a birefringent andradite-grossular from Crowsnest Pass. *Powder Diffr.* **2013**, *29*, 20–27. [CrossRef]

20. Phichaikamjornwut, B.; Skogby, H.; Ounchanum, P.; Limtrakun, P.; Boonsoong, A. Hydrous components of grossular-andradite garnets from Thailand: Thermal stability and exchange kinetics. *Eur. J. Mineral.* **2012**, *24*, 107–121. [CrossRef]

21. Quartieri, R.; Dalconi, S.; Boscherini, M.C.; Iezzi, F.; Boiocchi, G. Site preference and local geometry of Sc in garnets: Part I. Multifarious mechanisms in the pyrope-grossular join. *Am. Mineral.* **2006**, *91*, 1230–1239. [CrossRef]

22. Katiyar, J.K.; Sinha, S.K.; Kumar, A. Friction and wear durability study of epoxy-based polymer (SU-8) composite coatings with talc and graphite as fillers. *Wear* **2016**, *362–363*, 199–208. [CrossRef]

23. Kumaresan, K.; Chandramohan, G.; Senthilkumar, M.; Suresha, B.; Indran, S. Dry sliding wear behaviour of carbon fabric-reinforced epoxy composite with and without silicon carbide. *Compos. Interfaces* **2011**, *18*, 509–526. [CrossRef]

24. Marczak, J.; Kargol, M.; Psarski, M.; Celichowski, G. Modification of epoxy resin, silicon and glass surfaces with alkyl- or fluoroalkylsilanes for hydrophobic properties. *Appl. Surf. Sci.* **2016**, *380*, 91–100. [CrossRef]

25. Kang, Y.; Chen, X.; Song, S.; Yu, L.; Zhang, P. Friction and wear behavior of nanosilica-filled epoxy resin composite coatings. *Appl. Surf. Sci.* **2012**, *258*, 6384–6390. [CrossRef]

26. Hofmeister, A.M.; Mcaloon, B.P. Single-crystal IR spectroscopy of grossular-andradite garnets. *Am. Mineral.* **1995**, *80*, 1145–1156. [CrossRef]

27. Hofmeister, A.M.; Fagan, T.J.; Campbell, K.M.; Schaa, R.B. Single-crystal IR spectroscopy of pyrope-almandine garnets with minor amounts of Mn and Ca. *Am. Mineral.* **1996**, *81*, 418–428. [CrossRef]

28. Geiger, C.A.; Kolesov, B.A. Raman spectra of silicate garnets. *Phys. Chem. Miner.* **1998**, *25*, 142–151. [CrossRef]

29. Raymond, R.K.; White, W.B.; Long, T.V. Vibrational Spectra of the common silicate: I. The Garnets. *Am. Mineral.* **1971**, *56*, 54–71.

30. Bakirdere, S.; Yilmaz, M.T.; Tornuk, F.; Keyf, S.; Yilmaz, A.; Sagdic, O.; Kocabas, B. Molecular characterization of silver-stearate nanoparticles (AgStNPs): A hydrophobic and antimicrobial material against foodborne pathogens. *Food Res. Int.* **2015**, *76*, 439–448. [CrossRef] [PubMed]

31. Stan, M.S.; Constanda, S.; Grumezescu, V.; Andronescu, E.; Ene, A.M.; Holban, A.M. Thin coatings based on ZnO@C18-usnic acid nanoparticles prepared by MAPLE inhibit the development of Salmonella enterica early biofilm growth. *Appl. Surf. Sci.* **2016**, *374*, 318–325. [CrossRef]

32. Kim, K.; Lee, S.J. Diffuse reflectance infrared spectra of stearic acid self-assembled on fine silver particles. *Vib. Spectrosc.* **1998**, *18*, 187–201. [CrossRef]

33. Silva, A.M.T.; Nouli, E.; Carmo-Apolinário, Â.C.; Xekoukoulotakis, N.P.; Mantzavinos, D. Sonophotocatalytic/H_2O_2 degradation of phenolic compounds in agro-industrial effluents. *Catal. Today* **2007**, *124*, 232–239. [CrossRef]

34. Eswaramoorthi, I.; Sundaramurthy, V.; Das, N.; Dalai, A.K.; Adjaye, J. Application of multi-walled carbon nanotubes as efficient support to NiMo hydrotreating catalyst. *Appl. Catal. A Gen.* **2008**, *339*, 187–195. [CrossRef]

35. Fu, Z.; Su, L.; Liu, M.; Li, J.; Li, J.; Zhang, Z.; Li, B. Confinement effect of silica mesopores on thermal behavior of phase change composites. *J. Sol-Gel Sci. Technol.* **2016**, *80*, 180–188. [CrossRef]

36. Afkhami, M.; Hassanpour, A.; Fairweather, M.; Njobuenwu, D.O. Fully coupled LES-DEM of particle interaction and agglomeration in a turbulent channel flow. *Comput. Chem. Eng.* **2015**, *78*, 24–38. [CrossRef]

37. Senthilnathan, J.; Rao, K.S.; Lin, W.H.; Liao, J.D.; Yoshimura, M. Low energy synthesis of nitrogen functionalized graphene/nanoclay hybrid via submerged liquid plasma approach. *Carbon* **2014**, *78*, 446–454. [CrossRef]

38. Belon, C.; Schmitt, M.; Bistac, S.; Croutxé-Barghorn, C.; Chemtob, A. Friction and wear properties of hybrid sol-gel nanocomposite coatings against steel: Influence of their intrinsic properties. *Appl. Surf. Sci.* **2011**, *257*, 6618–6625. [CrossRef]

39. Bandeira, P.; Monteiro, J.; Baptista, A.M.; Magalhães, F.D. Magalhães, Influence of oxidized graphene nanoplatelets and [DMIM][NTf2] ionic liquid on the tribological performance of an epoxy-PTFE coating. *Tribol. Int.* **2016**, *97*, 478–489. [CrossRef]

40. Chang, L.; Zhang, Z.; Breidt, C.; Friedrich, K. Tribological properties of epoxy nanocomposites I. Enhancement of the wear resistance by nano-TiO_2 particles. *Wear* **2005**, *258*, 141–148. [CrossRef]

41. Dass, K.; Chauhan, S.R.; Gaur, B. Evaluation of mechanical, friction, and wear characteristics of nano-SiC filled ortho cresol novalac epoxy composites under dry sliding condition. *Adv. Polym. Technol.* **2015**, *34*, 21491. [CrossRef]

42. Hedayati, M.; Salehi, M.; Bagheri, R.; Panjepour, M.; Naeimi, F. Tribological and mechanical properties of amorphous and semi-crystalline PEEK/SiO_2 nanocomposite coatings deposited on the plain carbon steel by electrostatic powder spray technique. *Prog. Org. Coat.* **2012**, *74*, 50–58. [CrossRef]

43. Ozsoy, I.; Mimaroglu, A.; Unal, H. Influence of micro- and nanofiller contents on friction and wear behavior of epoxy composites. *Sci. Eng. Compos. Mater.* **2015**, *24*, 485–494. [CrossRef]

44. Wu, Y.; Yu, Z.; Liu, X. Tribological performance of in-situ epoxy composites filled with micro-sized ZrB_2 particles. *Compos. Part B* **2017**, *123*, 148–153. [CrossRef]

45. Yu, S.; Hu, H.; Ma, J.; Yin, J. Tribological properties of epoxy/rubber nanocomposites. *Tribol. Int.* **2008**, *41*, 1205–1211. [CrossRef]